Robustness assessment of multimodal freight transport networks

Zhidong He[a,*], Kumar Navneet[a], Wirdmer van Dam[b], Piet Van Mieghem[a]

[a]*Faculty of Electrical Engineering, Mathematics and Computer Science, Delft University of Technology, The Netherlands*
[b]*Rijkswaterstaat, The Netherlands*

Abstract

Multimodal freight transport allows switching among different modes of transport to utilize transport facilities more efficiently. This paper proposes an approach on network modeling and robustness assessment for multimodal freight transport networks, where the nodes represent junctions, terminals and crossings, and the links represent pathways. The network model captures the features of interconnection and interdependency. Freight can switch between different modalities at interconnected terminals, while disruption of a single interdependent node (e.g., bridge, tunnel, railway crossing) affects multiple modalities. Considering disruptions of infrastructure elements and capacity degradation of pathways as perturbations, the network robustness is evaluated as the increment of the total travel time caused by these perturbations. We apply our robustness assessment model to the Dutch freight transport, taking into account three modalities: inland waterway, road and railway. The node criticality, defined as the impact of a node removal on the total travel time, resembles a power-law distribution, independent of different traffic assignments. This scale-free property implies a relatively robust state of the network against single random disruptions. Further, we show that the most critical nodes can be roughly identified by their topological properties. Our research helps to schedule the maintenance by assigning priority to the critical infrastructure.

Keywords: Robustness assessment, Multimodal transport, Interdependency, Scale-free property

1. Introduction

The European hinterland freight transport sector has aimed at a shift towards multimodal transport such as railway, inland waterway and sea transport, in order to alleviate the saturation of road systems [1][2]. Intermodal transport and synchromodal transport are promoted as two promising solutions. Intermodal freight transport allows moving goods by using various modalities consecutively [3]. Synchromodal transport aims at real-time and flexible switching among different modes of transport according to the latest logistic information, so as to utilize all transport facilities more efficiently [4][5].

Transport networks are prone to suffer from various perturbations, for example infrastructure failures and temporary closures due to construction work. More severe perturbations, such as strikes or extreme weather (e.g. droughts, heavy snow, strong winds), could lead to the partial unavailability of transport networks. Network robustness is interpreted as a measure of the network's response to perturbations or challenges imposed on the network [6] [7], which considers both the network topology and the service for which the network is designed [8]. In transportation field, "Robustness" refers to the avoidance of direct and indirect economic losses of a transport network, which is defined as the degree to which the transportation network can function in the presence of various capacity disruptions on transport elements [9]. In the robustness analysis, evaluating the network performance reduction under network perturbations is a common approach. A more comprehensive review of related works refers to Section 2. Despite that many assessment approaches have been applied in different modes of transport, the framework of robustness assessment for multimodal

---

networks has seldom been studied [10]. The issues including *(i) how to abstract particular infrastructure (e.g. terminals and crossings) in multimodal transport? (ii) how to assess the network robustness under both structural disruptions and capacity degradation? (iii) what is the topological property of the traffic-based critical infrastructure element?* are still open. This study aims at addressing the above questions.

Introducing concepts of *Network Science* to transportation research allows us to propose a framework of network modeling, robustness assessment and critical structure identification for multimodal freight transport. The study of robustness in Network Science started with the critical percolation threshold in random graphs [11][12]. In recent years, the research issues emerging in Network Science, e.g., interdependent network [13], cascading failure [14], spreading process, percolation model, are receiving attention since these models of a high interpretability can feature more comprehensive behaviors in real-world networks, e.g., power grids, water distribution networks, congestion propagation. An interdependent network in Network Science is a multi-layer network consisting of different types of networks that depend upon each other for their functioning [13]. The interdependency in networks has been applied to measure the robustness of communication networks, that control and are supported by power grids [15], notably by investigating the impact of cascading failure [16][14]. The representation of interdependent networks is an excellent proxy for the structure of multimodal networks, which is first applied in transportation systems. Taking into account several modalities (e.g. inland waterway, road and railway), the transport infrastructure is modeled as a multilayered network, where the nodes represent junctions, terminals and crossings, and the links represent pathways. This network features two properties: interconnection [17] and interdependency [16]. Specifically, transloading terminals are facilities where freight can be transferred from one mode of transport to another and are modeled as interconnections. The crossings, whose functioning influences multiple modes of transport (e.g. bridges), are interdependent nodes. Thus, the disruption of a crossing implies a simultaneous unavailability of related pathways in multiple layers of the network. Consequently, this macroscopic network model abstracts the intricate connectivity of multimodal transportation networks, and also characterizes various types of network perturbations.

Based on the network model, we assess the robustness of multimodal transportation networks. We regard the total travel time of transporting all the freights as a performance indicator, which usually increases due to disruption of any infrastructure element [18]. Our framework assumes that the increment of total travel time due to a node removal reflects the criticality of this node. Then, the robustness of a network can be measured by considering the time increment arising from every node removal in a statistical way. The distribution of the nodal criticality in a large-scale network could provide insights on the evolution of transport behaviors. Further, we explore the correlation between the time increment due to a node removal and the topological properties of this node, which helps to identify the critical nodes faster.

We assess our approach by an extensive case study on the freight transport network in the Netherlands. The case study is not limited to the traffic assignment of all-or-nothing (AoN) [19], but also more practical traffic models, including modal split (MS) [20], user equilibrium (UE) [21] and system optimum (SO) [21]. We investigate the robustness performance and topological properties of the critical nodes under different traffic assignments. The assessment under single element disruptions identifies the critical nodes, whose disruption leads to a relatively high increment of the travel time. The critical nodes need to be given a higher priority for repairs and maintenance by the responsible organization. The robustness assessment under the capacity degradation of pathways can help to evaluate the impact of a large-scale disaster and work out contingency plans. A general recovery framework for any type of network is presented in [22], which allows to assess the performance of recovery measures in transport networks. One can refer to Project *RMTN*[1] on Github for the open source of our assessment framework and the cartographic data of our Dutch transport network. The main contribution of this work can be summarized as:

a. We introduce the concepts of interconnection and interdependency into modeling multimodal networks, which allow to evaluate the impact due to disruptions of the terminals and the crossings.
b. The framework of transport network assessment systematically considers disruptions/degradation of infrastructure under different traffic behavior.

---

[1]https://github.com/krnavneet1/RMTN

c. The assessment framework develops the method of roughly identifying critical nodes by nodal topological properties.

This paper is organized as follows. A short overview on related work is presented in Section 2. We introduce the method for modeling a multimodal transport network in Section 3. Section 4 proposes a framework of robustness assessment and defines a robustness indicator. We apply the assessment method to the Dutch freight transport network in Section 5. Section 6 summarizes our findings and concludes this paper.

2. Related work

There is a large body of related work on robustness/resilience of transport networks [23][24], which can be categorized according to transportation modes, robustness metrics and perturbation types.

2.1. Transportation modes

Due to different characteristics of various modes, previous research on robustness is categorized according to transportation modes including road network, freight transportation network, railway, waterway network, air network and multimodal transportation. This research focuses on multimodal/synchromodal transportation, which is in the agenda of the Dutch government and the Dutch Top Sector Logistics [25]. The main feature of multimodal/synchromodal transport includes a centralized management to monitor the traffic flow, to schedule the route of drivers and to allocate the cargo volume of vehicles, which helps to design a better traffic assignment and a more robust network [2]. As proposed by the Dutch Institute for Advanced Logistics (Dinalog), synchromodal transport entails that "A shipper agrees with a service operator on the delivery of products at specified costs, quality, and sustainability but gives the service operator the freedom to decide on how to deliver according to these specifications" [26]. The assumptions that (1) the freight from warehouses can be delivered from origin to destination via different modalities; (2) The quantity of freight from warehouses/regions can be divided into smaller units and carried by multiple vehicles/carriages/ships; allow the freight transport shares some similar traffic behaviors with urban traffic.

Comparing to single transportation modes, network modeling and robustness assessment of multimodal transport have not been studied extensively [2][24]. A network model of multimodal transportation processes was proposed to evaluate the network robustness allowing distinguished multimodal processes to continue in order to accomplish trips following an assumed set of multimodal chains [27]. A quantitative measure of resilience was employed to determine the best set of actions to improve security at critical components e.g., terminals and ports, in an intermodal network [28]. Chen *et al.* [29] built an integer programming model to obtain a quantitative measure of resilience of a port-hinterland container transportation from the perspective of shippers. Stamos *et al.* [30] presented a data-driven method for assessing the resilience of the European multimodal passenger transport network during extreme weather events. Darayi *et al.* [31] integrated a multi-commodity network flow formulation with an economic model to quantify the multi-industry impacts of a disruption in the network. The disruption management from passenger multimodal rerouting from airports due to the occurrence of perturbations on modes was considered in [32]. Although we have suffered the frequency occurrence and serious consequences of the crossings in transportation systems (e.g. 2019 Taiwan bridge collapses [2] and 2018 Amsterdam Highway tunnel collapses [3]), an approach for modelling and assessing the impact of disruptions of these crossings are still lacking.

2.2. Robustness metrics

The performance metrics applied for robustness assessment are divided into two aspects: topological metrics and traffic-based metrics. Topological metrics are usually constructed on some topological properties based on graph theory, such as size of giant component, average shortest paths, network diameter, network

---

[2]cnn.com/2019/10/01/asia/taiwan-bridge-collapse-intl-hnk-scli
[3]nltimes.nl/2018/01/03/ceiling-amsterdam-highway-tunnel-collapses

efficiency [33], which ignore specific traffic features. Traffic-based metrics (e.g. travel time [9], environmental cost [10]) reflect more functional and economic values, which are usually related to traffic assignment or operational attributes [24].

Since robustness measures the transport performance before and after disruptions of infrastructure elements, the infrastructure element (e.g., node or link) corresponding to the maximum performance reduction is the critical component. Several approaches on identifying the critical component are proposed based on either topological properties (e.g., degree centrality, closeness centrality, betweenness centrality, eigenvector centrality) or predisaster traffic-based simulations [31][34][35]. However, seldom insights have been presented on the topological properties of the critical nodes identified by traffic-based assessment approaches. Our work aims to explore this issue in the transportation field.

2.3. Perturbation types

The perturbation on transport networks can be categorized into two variants: connectivity-related and capacity-related. Connectivity related perturbations [36, 37, 38] regard the failure of infrastructure elements as removed nodes/links from a network. Capacity-related perturbations [39, 9, 40, 41] consider failures of infrastructure elements as the capacity reduction of parts of the network, as opposed to an entire removal of parts of the network.

In this paper, we consider two types of real-world perturbations: disruptions of single infrastructure element and extreme weather events. We assume that the disruption of one node implies an entire of unavailability of this infrastructure element and its blockage for safety, which belongs to the connectivity-related perturbations. The impact of extreme weather events usually leads to the partial unavailability of transport networks [30][42], which corresponds to the capacity reduction of this transport mode (e.g., low river level degrades riverway capacity, heavy snow degrades road capacity). Further, our proposed framework allows us to consider these two types of perturbations simultaneously, i.e., identifying critical nodes under extreme weather.

3. The synchromodal network model

In this section, we briefly introduce the network model for multimodal transport, which features multiple layers, interconnection and interdependency. We refer to our previous report [43] for supplementary information about the infrastructure considered and the network modeling.

3.1. Multi-layer network

The underlying topology of the multimodal freight transportation can be represented by an undirected network $G(\mathcal{N}, \mathcal{L})$ with the set $\mathcal{N}$ of N nodes and the set $\mathcal{L}$ of L links. The nodes in the network represent transloading terminals, crossings and junctions, which are connected by the links as different types of pathways. In our network model (as illustrated in Figure 1), we consider three modalities: road (Road), railway (Rail) and inland waterway (Water), which are the most common modalities in many European countries. The underlying topology of each modality is represented by a subgraph $G_m(\mathcal{N}_m, \mathcal{L}_m)$ for modality $m \in \{Road, Rail, Water\}$. The terminals providing the interconnection between different modalities are represented by the subgraph G_T, and the origins and destinations (OD) locating the sources and targets of cargo demands are defined in the subgraph G_{OD}. The whole transport network is a supergraph which consists of multiple undirected subgraphs. Thus, the resulting supergraph combining all infrastructure elements is defined as $G(\mathcal{N}, \mathcal{L})$ with node and link set,

$$\mathcal{N} = \mathcal{N}_{Road} \cup \mathcal{N}_{Rail} \cup \mathcal{N}_{Water} \cup \mathcal{N}_T \cup \mathcal{N}_{OD} \tag{1}$$

$$\mathcal{L} = \mathcal{L}_{Road} \cup \mathcal{L}_{Rail} \cup \mathcal{L}_{Water} \cup \mathcal{L}_T \cup \mathcal{L}_{OD} \tag{2}$$
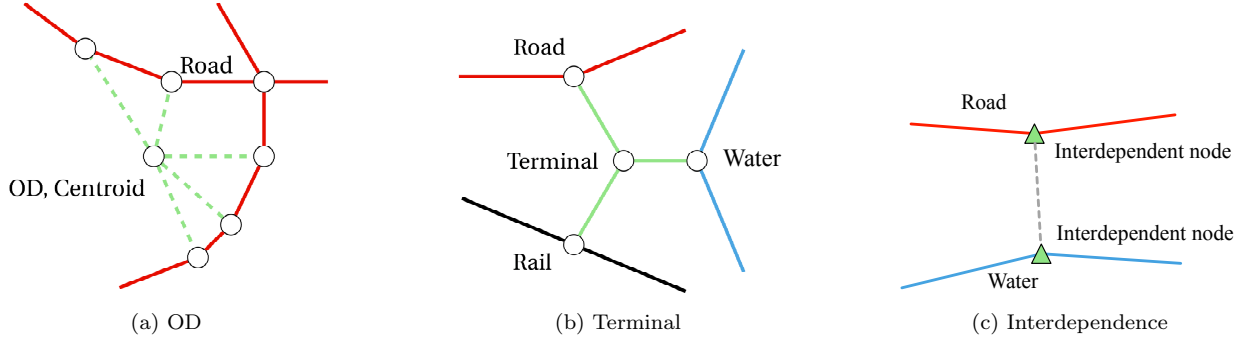
4

Figure 1: Illustration of network modeling. (a) Connections between OD centroid and main roads. Solid lines represent main roads, and green lines represent small roads. (b) Connections between terminal and main roads of modalities. Green lines represent small roads. (c) Relation between two modalities with an interdependent node. The solid lines represent main pathways and the grey dash line represents the interdependent relation between node pairs.

3.2. Origins and destinations (OD centroid)

Centroids of regions are used [10] [44] to model the origins and destinations in each region, where the centroid of a polygonal area is located at the center of mass of that polygon. We split the country into several regions, where the centroid of each region represents the origin and destination of the freight transport demand in that region. For example, we apply the centroids of NUTS-3 regions[4] (a statistical subdivision of Europe) as the OD centroid in our case study. Each centroid also represents the cargo demand of this region, which can abstract a storage facility of freight in actual transport networks. These centroids are represented by the nodes in the subnetwork G_{OD}. We assume that the centroid is connected to all access points in the road subgraph of this region by small roads. The small roads are represented by the OD links in the subnetwork G_{OD}. Figure 1a illustrates the network model for centroids.

The amount of freight (in tons) that is transported between the origins and destinations is defined in the demand matrix D, where the element D_{ij} defines the average amount of cargo transported from region i to region j. Freight transported between the origin and the destination in the same region is not considered, and thus the diagonal elements of the demand matrix D are all equal to 0.

3.3. Interconnection

Intermodal transport allows switching among different modes of transport at transloading terminals. At a transloading terminal two or more modalities are interconnected. The containers can be transshipped in container terminals (sometimes called inland ports). We take three types of container terminals (i.e. rail terminals (connecting Rail and Road), waterway terminals (connecting Waterway and Road) and trimodal terminals (connecting all three modalities)) into account. Figure 1b illustrates the network model for these terminals. Each transloading terminal is represented by a node in the subgraph G_T. The terminal node is connected with links to nodes of the appropriate modes of transport. This modeling method captures the feature of disruptions of terminals, i.e. the freight cannot switch to a different mode of transport if the terminal node is removed.

3.4. Interdependency

The three modalities (waterway, road and rail) cross each other regularly (see Figure 3 below). At each crossing, a civil engineering structure is needed (e.g. bridge, tunnel, railway crossing) to efficiently use both modalities. Thus, the disruption of a single civil engineering structure can affect multiple modalities, which causes the interdependency between the modalities. For example, the disruption of a bridge can affect both

---

the road and the waterway simultaneously. Unlike for interconnection, transloading of freight is not possible at these crossings. Figure 1c illustrates the network model of an interdependent node. We represent each crossing structure as two nodes in the subgraphs of the two modalities. The relation of interdependency between these two nodes implies a simultaneous removal due to a disruption, i.e. if either node is removed, the other node will be removed as well.

4. Network robustness assessment

Our robustness assessment will be described in detail in this section based upon Figure 2. The proposed framework encompasses two aspects: the infrastructure designed by network operators and traffic behavior determined by drivers, which corresponds to the fact that the network robustness is related to its underlying topology and services [8]. For the transport network, we can compute the predefined performance indicator of the fully-functional network based on specific OD-demands and a given traffic assignment. Both the degradation of the functionality of pathways and the disruptions of transport elements could change the network performance indicator (i.e. the total travel time). For the same OD demands and the same traffic assignment, we recompute the performance indicator in the perturbed network. We then assess the robustness of the whole network based on the changes of the performance indicator due to the perturbations. The framework provides the method for exploring the relation between the impact of the disrupted elements on the performance and several topological properties of these elements.
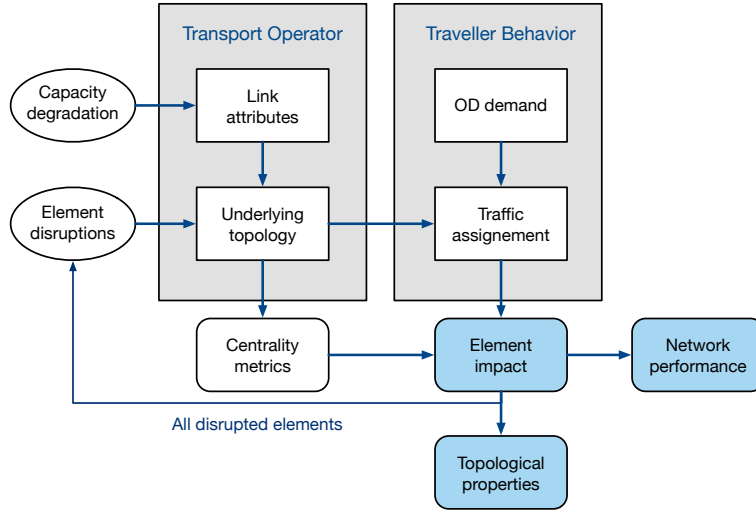

Figure 2: Framework of transport network assessment

4.1. Link attributes

The performance of the transport system is related to the route condition of each modality, which translates to the link attributes in the network model. Each pathway segment represented by a link ℓ in the network has two attributes: the free-flow average speed v_ℓ (in kilometers/hour) and the capacity c_ℓ (in tons/hour). The average speed v_ℓ (in kilometers/hour) determines the travel time t_ℓ (in hours) on link ℓ, i.e. $t_\ell = \frac{d_\ell}{v_\ell}$, where d_ℓ is the length of link ℓ (in kilometers). Considering the travel time as the cost of freight transportation, the travel time t_ℓ is regarded as the link weight in the network for computing the shortest path from the origin to the destination.

The average speed v_ℓ is a constant for the traffic assignments without capacity constraint, i.e. the link travel time t_ℓ is also constant for any amount of flow x_ℓ (in tons/hour) assigned on the link ℓ. In contrast, the link capacity constraints are included in the travel time functions considering traffic congestion. A popular

form of these functions that reflects the travel time $t_\ell(x_\ell)$ for each vehicle as a function of the flow x_ℓ (in tons/hour) on link ℓ, proposed by the Bureau of Public Roads (BPR), is given by [19]:

$$t_\ell(x_\ell) = t_{0\ell}\left(1 + \alpha\left(\frac{x_\ell}{c_\ell}\right)^\gamma\right) \tag{3}$$

where c_ℓ is the capacity of link ℓ (in tons/hour), and $t_{0\ell} = \frac{d_\ell}{v_\ell}$ is the free flow travel time, α and γ are the shape coefficients, for which the value of $\alpha = 0.15$ and $\gamma = 4$ are generally applied [19]. The travel time t_ℓ without considering congestion is consistent with an infinite link capacity $c_\ell \to \infty$.

4.2. Network perturbation

Network perturbations refer [22][45] to two scenarios: the disruptions of transport elements and the degradation of capacity, which translate to the changes in the underlying topology and the link attributes, respectively. For the scenario of node disruptions, the unavailable nodes are regarded to be removed from the original underlying topology. In this paper, we mainly consider disruptions of individual nodes to investigate the impact of each node on the performance of the network. This analysis may help to identify the critical infrastructure elements and schedule improvement measures. The scenario of node disruptions also includes the case that multiple nodes can be removed simultaneously, which describes simultaneous accidents or cascading failures [16]. We define a *random failure* as the failure scenario where a given fraction of multiple elements are removed from the network uniformly at random [22].

The scenario of capacity degradation refers to the effect of capacity reduction of a single modality on the performance of the whole network. This scenario aims to describe the cases of large-scale natural and man-made disasters, e,g. driver strikes and low water levels in rivers due to droughts.

4.3. Performance indicator

We denote by z_ℓ the total amount of freight (in tons) attempting to use link ℓ as the flow rate x_ℓ (in tons/hour) within h hours, i.e., $z_\ell = x_\ell h$. Invoking that the delay time for each vehicle traveling on link ℓ is t_ℓ specified by (3), we apply the total travel time, also called the total delay time, C_G (in tons·hours) of transporting all the freights among all links to measure the performance of network G, which is defined as

$$C_G = \sum_{\ell \in \mathcal{L}} z_\ell t_\ell(x_\ell) \tag{4}$$

The network performance indicator C_G usually increases to $C_G + \Delta C_G$ due to node disruptions and degradation of link attributes. The robustness can be measured by the normalized increment of the total travel time due to the perturbation on the network, which defines the robustness indicator η_G as

$$\eta_G = \frac{C_{G'} - C_G}{C_G} = \frac{\Delta C_G}{C_G} \tag{5}$$

where G' is the network after perturbations.

For measuring the impact of a single node disruption on the performance of the network, we define the *node criticality* as the normalized increment of the total time caused by the node removal. The node criticality is similar to the network robustness index proposed by Scott *et al.* [46]. The node criticality of node i is the same as the robustness indicator η_G under the single node disruption, which is

$$\omega_i = \frac{C_{G\setminus\{i\}} - C_G}{C_G} \tag{6}$$

where $G\setminus\{i\}$ is the graph in which node i is removed as well as all its incident links. The network robustness under isolated single disruptions can be measured by the average node criticality $E[\omega] = \frac{1}{N}\sum_{i=1}^{N}\omega_i$ among all nodes. In general, a smaller average node criticality $E[\omega]$ implies a more robust network.

4.4. Traffic assignment

We investigate four kinds of traffic assignments: all or nothing, modal-split logit model, user equilibrium and system optimum.

4.4.1. All or nothing (AoN)

An all-or-nothing (AoN) assignment is commonly applied for traffic assignment in networks. The AoN assignment in this paper assigns all demand of each OD pair to the route with the lowest route time between the OD pair [10][47], where the link weight is the free-flow travel time $t_{0\ell} = \frac{d_\ell}{v_\ell}$. Two limits of the AoN algorithm are: (1) the capacities c_ℓ of the pathways are assumed to be infinite; and (2) the diversity of route choices for each OD pair is not taken into account. Despite the limits of the AoN assignment, the operational simplicity without extra parameters leads to rapid computation, which allows to roughly understand traffic behaviors under low-loaded situations. The shortest routes are computed by the Bellman-Ford algorithm [48] in our framework.

4.4.2. Modal-split assignment (MS)

Modal-split assignment also assumes the infinite link capacity c_ℓ. The demands between origins and destinations are distributed over the network by applying a probabilistic route choice model in modal-split assignment [20]. The freight between the origin and the destination is distributed over several different routes in the route choice set by using a multinomial logit regression. Given the routes set $\mathcal{P}_{sd}$ with the first $|\mathcal{P}_{sd}| = K$ shortest paths from origin s to destination d, the fraction of freight using the k-th route $\mathcal{P}_{sd,k}$ is defined as

$$p_{sd,k} = \frac{\exp\left(-\beta t(\mathcal{P}_{sd,k})\right)}{\sum_{k \in K} \exp\left(-\beta t(\mathcal{P}_{sd,k})\right)} \tag{7}$$

where $t(\mathcal{P}_{sd,k})$ is the total time along the route $\mathcal{P}_{sd,k}$ alone and β is the parameter tuning the drivers' preference for the route with a lower travel time. The total flow assigned to link ℓ follows

$$x_\ell = \sum_{s \in \mathcal{N}} \sum_{d \in \mathcal{N}} \sum_{k \in \{1,2,...,K\}} D_{sd} \cdot p_{sd,k} \cdot \delta(\mathcal{P}_{sd,k}, \ell) \tag{8}$$

where $\delta(\mathcal{P}_{sd,k}, \ell)$ takes the value one if link ℓ is belong to the route $\mathcal{P}_{sd,k}$ and zero otherwise.

4.4.3. User equilibrium (UE)

According to Wardrop's first principle [49], drivers in a congested network prefer choosing their route selfishly, following a behavior that is captured by the Nash equilibrium of the underlying non-cooperative game. Assuming that the driver has perfect knowledge of the travel time on a network and able to choose the best route according to Wardrop's first principle [50], the behavioral assumption will lead to a deterministic user equilibrium. Using a potential function $\phi_\ell(x_\ell) = \int_0^{x_\ell} t_\ell(x)dx$, this routing behavior minimizes the sum of the potential functions, which is formulated as a convex optimization problem:

$$
\begin{aligned}
\underset{x_\ell \forall \ell \in L}{\text{minimize}} \quad & \sum_{\ell \in \mathcal{L}} \int_0^{x_\ell} t_\ell(x)dx \\
\text{subject to} \quad & \sum_{\mathcal{P}} f_{\mathcal{P}}^{sd} = \frac{D^{sd}}{h} \\
& x_\ell = \sum_s \sum_d \sum_{\mathcal{P}} f_{\mathcal{P}}^{sd} \delta^{sd}(\mathcal{P}, \ell) \\
& x_\ell \geq 0, f_p^{sd} \geq 0.
\end{aligned}
\tag{9}
$$

where x_ℓ is the total flow on link ℓ, $f_{\mathcal{P}}^{sd}$ is the flow between origin s and destination d on route $\mathcal{P}$, and the indicator $\delta^{sd}(\mathcal{P}, \ell) = 1$ if link ℓ belongs to route $\mathcal{P}$, and $\delta^{sd}(\mathcal{P}, \ell) = 0$ otherwise. The above traffic assignment problem can be solved by the Frank-Wolfe algorithm [51]. The total travel time in the UE assignment is computed using $C_G = \sum_{\ell \in L} x_\ell^* h \cdot t_\ell(x_\ell^*)$ where x_ℓ^* is the solution of problem (9).

4.4.4. System optimum (SO)

System optimum assignment follows Wardrop's second principle, where drivers cooperate with each other to minimize the total travel cost [21] of the whole transport system. The flow configuration that results in the optimal total travel time refers to the socially optimal flows obtained by the problem:

$$\underset{x_\ell \forall \ell \in L}{\text{minimize}} \quad C = \sum_{\ell \in L} x_\ell h \cdot t_\ell(x_\ell) \tag{10}$$

$$\text{subject to} \quad \text{constraints in (9)}.$$

which also can be solved by a modified FrankWolfe algorithm. The total travel time in the SO assignment is computed by $C_G = \sum_{\ell \in L} x_\ell^* h \cdot t_\ell(x_\ell^*)$ with the solution x_ℓ^* of problem (10). Some previous works have discussed the relation between the UE and the SO [52][53], which propose that a trade-off between the UE and the SO agrees more with the real-world traffic behaviors. Beyond this paper, the sensitivity analysis for the UE and the SO with respect to topological changes may help to compute the flow on each link in a perturbed network more rapidly [54][55].

5. Case study: the Dutch container freight transport network

5.1. Network model and configuration

5.1.1. Underlying topology

We apply the NWB (*Nationaal Wegenbestand*) database to construct the transport network. The NWB is made by Rijkswaterstaat and defines the section and intersections for all public roads[5], waterways[6] and railways[7] in the Netherlands. For each mode of transport a subset of the network is used. Only the large waterways, the railways that are regularly used for freight transport and the national roads are considered for the network. The terminal nodes are defined in the Rijkswaterstaat documents[8][9][10], while the interdependent crossings are located manually according to Google map. Figure 3 illustrates the transport network of the Netherlands.

The Netherlands is divided into 40 regions (NUTS-3 used by Eurostat[11]) based on BasGoed[12], each of which is represented by a centroid node. Figure 4 illustrates the amount of containers transported from and towards all regions in the Netherlands, which determines the OD demand matrix D. We assume that all the freights enter the traffic system in the peak period within one hour, i.e., $h = 1$. The Dutch freight transport network consists of 1457 nodes, 44 terminals, 40 centroids, 1897 main-pathway links, 101 terminal links and 692 OD links.

5.1.2. Link attributes configuration

We assume that the travel time of road, railway and waterway has a similar behavior. More specifically, the travel time is nearly a constant under low-flow conditions, while the travel time increases sharply for the high flow approximating the path capacity under congested conditions. For simplicity without loss of generality, we apply the BPR function (3) to feature the above characteristic where the parameters can tune the behavior of different modalities. Different modalities yield different configurations of link attributes in

---

[5]Rijkswaterstaat, Nwb-wegen [roads], 2017. URL: https://www.pdok.nl/nl/ service/wfs-nwb-wegen-nationaal-wegen-bestand.

[6]Rijkswaterstaat, Nwb-vaarwegen [waterways], 2017. URL: https://www.pdok.nl/nl/service/wfs-nwb-wegen-nationaal-vaarwegen-bestand.

[7]Rijkswaterstaat, Nwb-spoorwegen [railways], 2017. URL: https://www.pdok.nl/nl/service/wfs-nwb-spoorwegen-nationaal-wegen-bestand.

[8]ECORYS Nederland BV. Intermodal links - planner, 2017. URL: https://intermodallinks.com/Planner/.

[9]Port of Rotterdam. Inlandlinks, 2017. URL:https://www.inlandlinks.eu/nl/terminals/filter.

[10]Rijkswaterstaat. Synchromodaal transport Nederland kaart [synchromodal transport Netherland map], 2017. Internal document.

[11]European Commission. Nuts - nomenclature of territorial units for statistics, 2017. URL: ec.europa.eu/eurostat/web/nuts.

[12]Rijkswaterstaat, Basgoed [model for freight transport], Internal model, 2017.

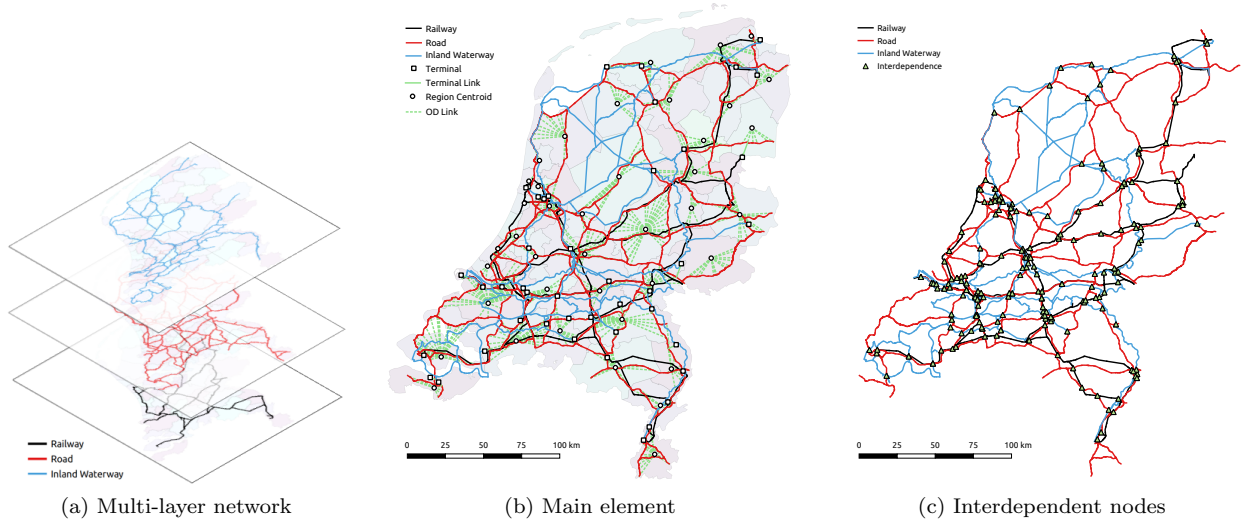(a) Multi-layer network   (b) Main element   (c) Interdependent nodes

Figure 3: Illustration of underlying topology of the freight transport network in the Netherlands. (a) Multi-layered network with three modes of transport. (b) Map of main infrastructure elements. (c) Location of the interdependent nodes.

each layer of the network in Figure 3a, which define the parameters (i.e., the parameter α, γ, the average speed v_ℓ, the capacity c_ℓ) in the BPR function (3) for each link. Table 1 presents the link attributes used. The small roads between OD/terminals have a lower average speed than the main roads. Compared with the Road and the Water, the travel time for the Rail depends more on the capacity of the railway, as the maximum number of trains on a railway is predetermined. Therefore, we set a large γ for the Rail. This means the travel time t_ℓ per unit of freight increases little with the freight amount below the capacity, but increases a lot for the amount above the capacity. The information about the average speed and the capacity of each modality is provided in the reports[13][14][15].

Modality	α	γ	v_ℓ	c_ℓ
Road (main)	0.15	4	60	2300(vehicle/hour)$\times$2(tons/vehicle)
Road (small)	0.15	4	30	2300(vehicles/hour)$\times$2(tons/vehicle)
Rail	0.15	8	90	2200(tons/train)$\times$2(trains/hour)
Water	0.15	4	15	1200(tons/ship)$\times$5(ships/hour)

Table 1: The configuration of the links attributes, including the parameters α and γ, the average speed v_ℓ (in kilometers/hour), and the capacity c_ℓ (in tons/hour).

5.2. Robustness assessment under random failures

We next investigate the robustness performance of the network under random failures. Under the scenario of random failure, we remove a fraction of nodes uniformly at random from the network, then compute the increment of the total travel time ΔC_G due to the removals. The ratio of the increment travel time and the original travel time referring to (5), i.e., $\eta_G = \frac{\Delta C_G}{C_G}$, is used to measure the robustness of a transport network. Figure 5 shows the average indicator $E[\eta_G]$ among all realizations of random node removals under the AoN assignment. The interconnection of multiple modalities can decrease the average normalized increment of

[13]CBS, Transport of goods in the Netherlands hits new record, 2016. URL: https://www.cbs.nl/en-gb/news/2016/25/transport-of-goods-in-the-netherlands-hits-new-record.

[14]ProRail, Network statement 2019, report T20160098-1656408669-827, p. 196, 2017.

[15]Statline, Traffic intensity; national roads, 2018. URL: https://opendata.cbs.nl/statline/CBS/nl/dataset/82855NED.
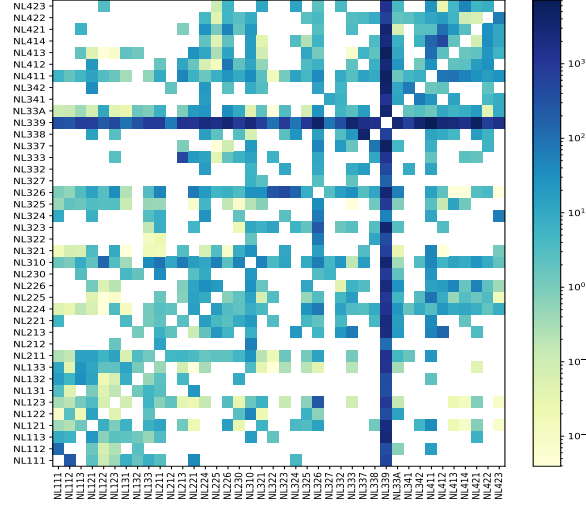
Figure 4: Demand matrix D for the amount of containers (in tons per business day) transported in the Netherlands (domestic transport only). The data is from BasGoed.

the total travel time $E[\eta_G]$, thus improves the robustness for transport services against random failures. Meanwhile, the interdependency effect of the crossing nodes between different modalities could degrade the robustness indicator $E[\eta_G]$ sightly, which is due to the fact that the failure of an interdependent node impacts two modalities simultaneously. Thus, we observe from Figure 5 that the interconnection improves the robustness and the interdependency degrades the robustness under random failures.
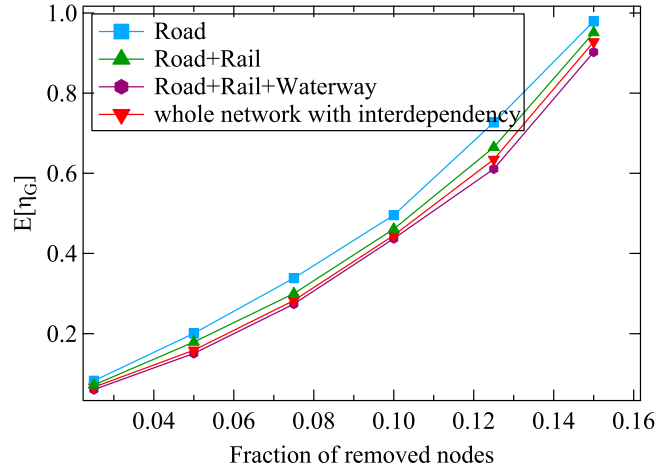

Figure 5: The average robustness indicator $E[\eta_G]$ under random failures as a function of the fraction of removed nodes. We compare four cases: (1) the Road, (2) the Road interconnected with the Rail, (3) three interconnected modalities without the interdependent nodes, (4) the whole network. Each data point is based on 100 realizations.

5.3. Robustness assessment via node criticality

Next, we investigate the distribution of the node criticality ω for all nodes and the interdependent nodes. Figure 6 shows the probability density function (PDF) $f_\omega(w)$ of the node criticality ω as random variables on log-log scale. We fit the distribution of the node criticality ω_i by a power-law PDF that $f_\omega(w) \sim w^{-k}$. We observe from Figure 6 that the node criticality resembles a power-law distribution, where different traffic
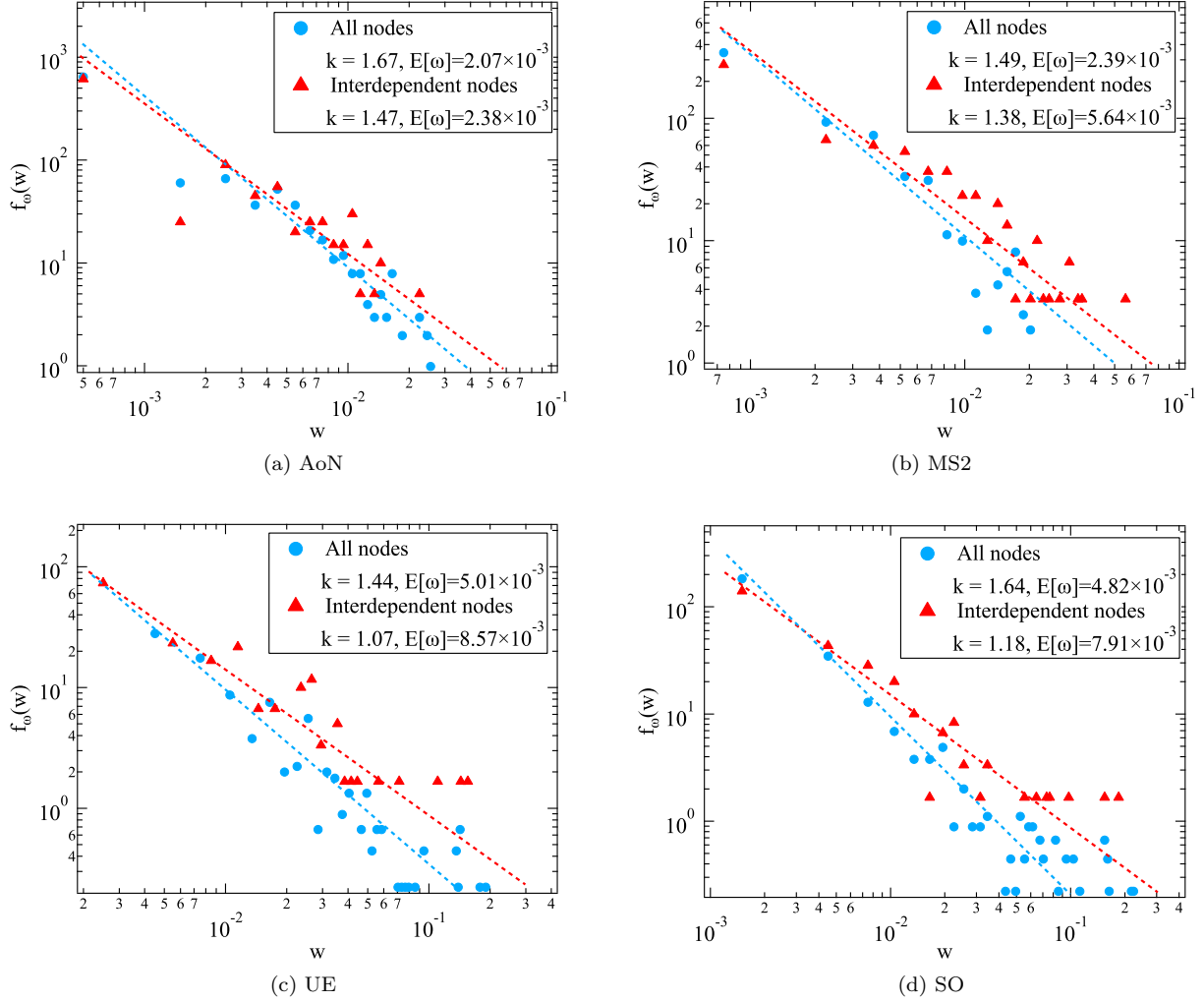
11

Figure 6: Distribution of the node criticality ω for both all nodes and the interdependent nodes. The PDF is fitted by the function $f_\omega(w) \sim w^{-k}$. Both the x-axis and y-axis are on log scales.

assignment models, i.e., the AoN, the MS2 (i.e. the modal split assignment with $K = 2$ routes), the UE and the SO, have little influence on this scale-free property of robustness. The power-law distribution of the node criticality ω_i implies that the removal of most nodes yields a small increment of the total travel time ΔC_G, while the removal of some critical nodes can increases the travel time C_G significantly. Interestingly, the real-world transport network already tends to be robust against individual failures, which may be caused by the topological evolution [56] and traffic optimization during the development of the network.

A larger slope k in the PDF $f_\omega(w) \sim w^{-k}$ implies a better robustness indicated by the node criticality ω of network. Comparing the traffic assignment AoN and the MS2, both with an infinity capacity, the AoN surprisingly presents a better performance against single failures with a larger slope k than the MS2. The AoN employs fewer nodes than the MS2, so that some removed nodes have little influence on the increment of the total travel time ΔC_G. Comparing the UE and the SO, the robustness indicated by the distribution of the node criticality ω under the SO outperforms the UE for disruptions among both all nodes and the interdependent nodes. This implies that a centralized and information-sharing schedule could lead to both a lower total travel time C_G and a better robustness $E[\omega]$. In addition, Figure 6 shows that the interdependent

nodes usually have a higher node criticality among all nodes. Thus the maintenance of the interdependent nodes should be of a higher priority.
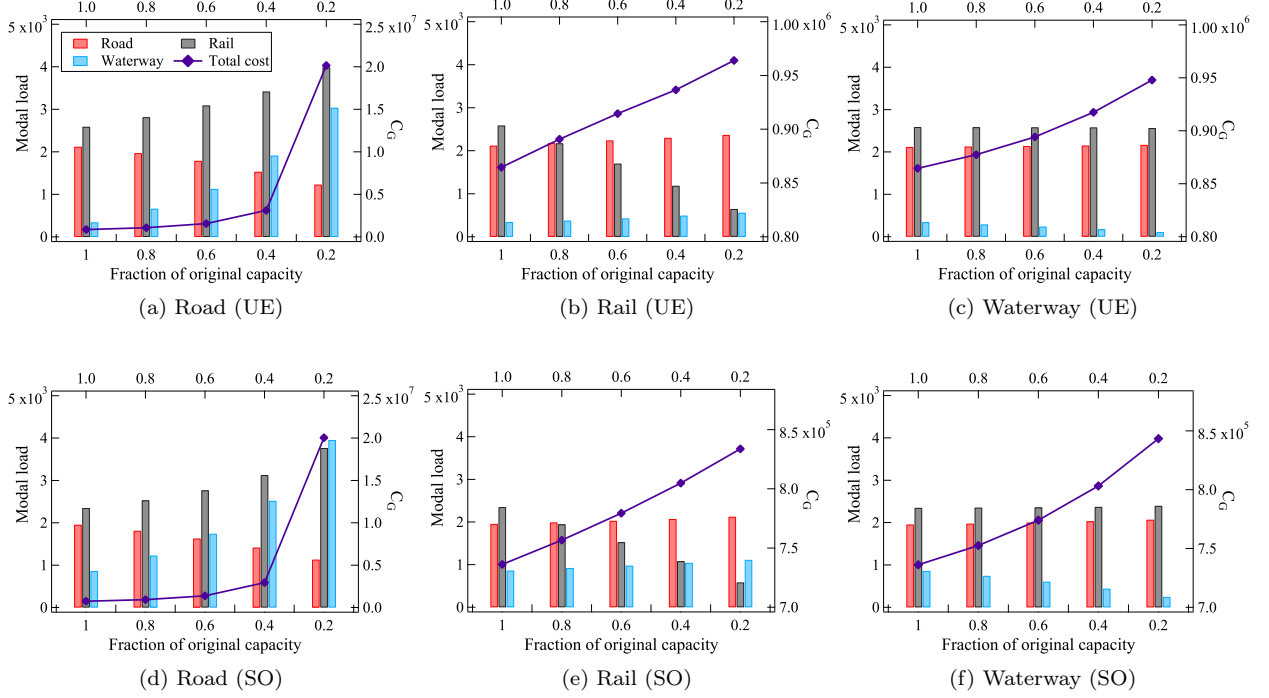

Figure 7: Bar plots show the modal load versus the fraction of the original capacity of a determined modality (the Road, the Rail or the Waterway) and a given traffic assignment (the UE or the SO). The purple lines show the total travel time C_G as a function of the fraction of the original capacity

5.4. Robustness assessment under capacity degradation

We further investigate the robustness of networks under capacity degradation. First, we define the modal load χ_m as the total flow $\sum_{\ell \in \mathcal{L}_m} x_\ell$ on all the links in this modality divided by the number of links L_m of this modality, i.e. $\chi_m = \frac{\sum_{\ell \in \mathcal{L}_m} x_\ell}{L_m}$, which reflects the usage of each modality. Figure 7 shows the modal load χ_m and the total travel time C_G versus the degradation of the capacity of each modality. The degradation of the capacity of a modality decreases the modal load of this modality, while the load shifts to the other two modalities. For the Rail and the Waterway, the total time C_G presents a linear function of the fraction of the original capacity, while the degradation of the Road capacity increases the total travel time C_G sharply. The high sensitivity of the total travel time C_G with the capacity degradation of the Road may be due to the fact that the Road is the dominating modality, and the other two fail to balance the loads if the availability of the Road decreases too much. Figure 7 also shows that the SO presents a lower travel time C_G than the UE due to the difference in the usage of Waterway, i.e., the SO has a higher modal load of the Waterway than the UE. This result hints a possible optimization for transportation by making full use of the Waterway.

We consider the single node disruption under capacity degradation of each modality. Figure 8 shows the average node criticality $E[\omega]$ as a function of the fraction of the original capacity for each modality, which measures the robustness against single disruption under degradation of capacity. The average node criticality $E[\omega]$ increases with degradation of the capacity of the Road and the Railway and more sensitive to degradation of the Road capacity. By contrast, the average node criticality $E[\omega]$ presents different behaviors

for the degradation of the Rail capacity, which more or less presents a Braess's paradox [57], i.e. the robustness degrades for a higher capacity of the Rail.
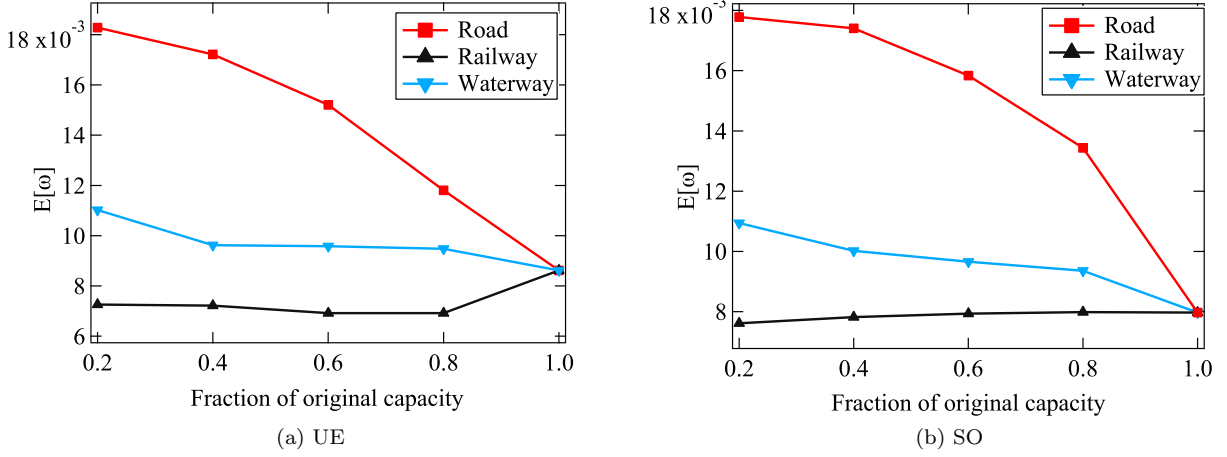

Figure 8: The average node criticality $E[\omega]$ as a function of the fraction of the original capacity for each modality under the UE and the SO.

5.5. Topological properties of critical nodes

We investigate the relation between the nodal topological properties and the node criticality in order to identify the most vulnerable and critical nodes faster [58]. A larger absolute correlation coefficient implies a better nodal metric to identify the critical node. The metric of the unweighted degree is the number of links incident to a node, and the other metrics (i.e. degree, closeness [59], node betweenness [59] and the diagonal element of the pseudo-inverse matrix [60] of the weighted Laplacian matrix $Q_{ii}^{\dagger}$) are computed in the weighted network with the link weight $a_\ell = t_{0\ell} = \frac{d_\ell}{v_\ell}$. The element $Q_{ii}^{\dagger}$ is calculated by the Laplacian matrix $\tilde{Q}$ of the weighted adjacency matrix $\tilde{A}$ with entry $\tilde{a}_\ell = \frac{1}{a_\ell}$ for each link ℓ. Figure 9 shows that the betweenness has the highest rank correlation with the node criticality, but the correlation degrades under the MS2, the UE and the SO assignments. Considering that the UE and the SO are more practical in real-world, this degradation implies that the identification of the critical nodes could be difficult if the effect of capacity is taken into account under the UE and the SO.

We define the flow network as the network with the link weight $a_\ell = x_\ell$ and denote the corresponding metrics by *. The flow network reflects the usage of each link under a specific traffic assignment. The unweighted degree* in the flow network is the number of non-empty links (i.e. $x_\ell \neq 0$) incident to a node. The other metrics are computed in the weighted flow network. The degree* in the flow network is actually the total amount of freight passing this node, which becomes the best indicator of the critical nodes. However, the rank correlation also degrades in the MS2, the UE and the SO, which implies that the critical nodes do not entirely depend on the local traffic flow.

We also investigate the topological properties of critical interdependent nodes. Since the closeness* is calculated as the reciprocal of the sum of the length of the shortest paths between the node and all other nodes in the flow network [59], the important nodes nearby the links with a high link weight $a_\ell = x_\ell$ usually have a smaller closeness*, which leads to the negative correlations between the node criticality and the closeness*. Figure 9 shows that the interdependent nodes present similar behavior of the topological properties with all nodes, but have a higher correlation with the closeness*. The strong correlation allows us to identify the most critical interdependent nodes by using the degree* and the closeness* in combination.
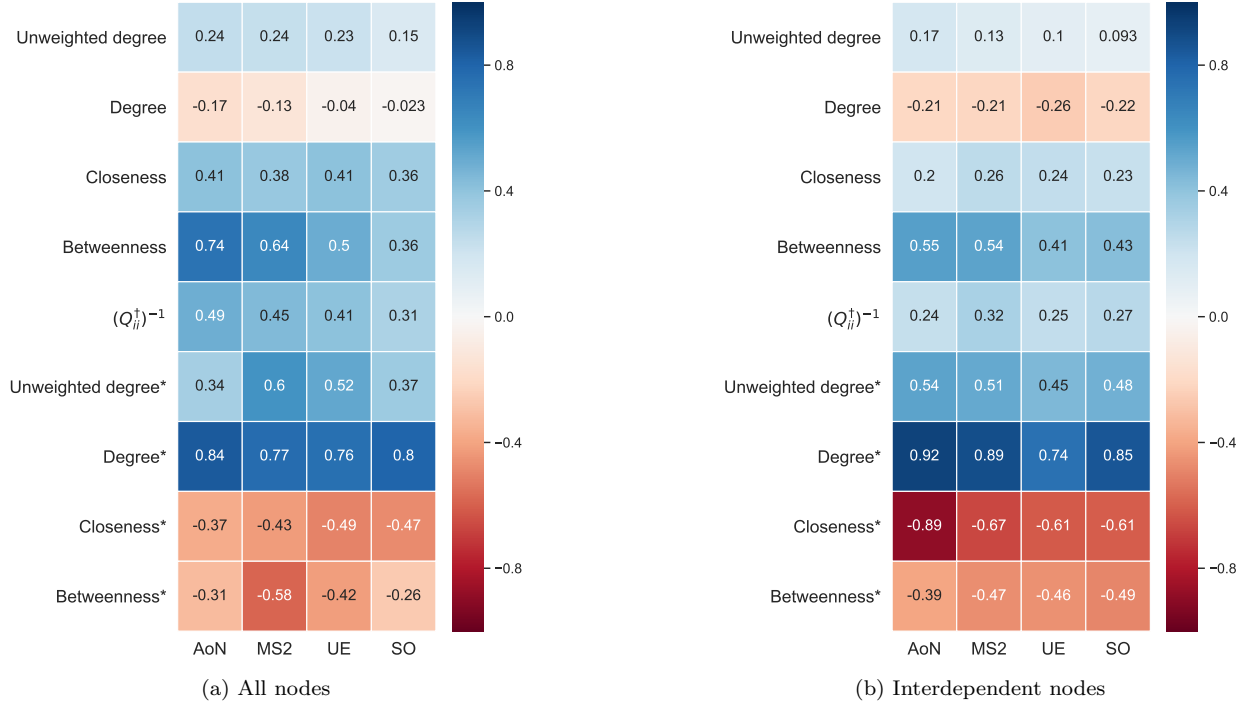
14

Figure 9: The Spearman's rank correlation coefficients between the node criticality and the topological metrics in the structural network (with $a_\ell = t_{0\ell}$) and the flow network (with $a_\ell = x_\ell$) under different traffic assignments. The coefficients for (a) all nodes and (b) the interdependent nodes are shown in the subgraphs, respectively. We neglect the element $Q_{ii}^{\dagger*}$ in the flow network since the weighted adjacency matrix $\tilde{A}$ is not applicable for the network with zero-weighted links $a_\ell = x_\ell = 0$.

6. Conclusion

Multimodal transport opens a new door for mitigating congestion in road transport and for reducing transportation costs. This paper addresses the approaches to both the network modeling and the robustness assessment of multimodal transport networks. The consideration of the interdependent property of multimodal networks fills the gap for modeling the disruptions of the crossings. Although the interdependency degrades the robustness of the network slightly, the interconnection of multiple modalities benefits the total travel time and outweighs the negative effect of interdependency on the robustness performance. The robustness is assessed by both element disruptions and capacity degradation. The case study of the Dutch transport network provides several new insights. First, the power-law-like distribution of the node criticality implies a good robustness of the real-world network. The dynamics of self-evolution and overall planning leading to this robust state could be an open question beyond this paper [61]. Second, we observe that the capacity degradation of the Road could exert a disastrous growth of the total travel time, while shifting more loads to the inland waterways can decrease the total travel time. Lastly, the node criticality is strongly correlated to the amount of freight passing this node. The most critical interdependent node can be identified by the degree and the closeness of nodes in the flow networks. This study can support network planners in tactical and operational decisions for improving the performance of multimodal transport networks.

The proposed framework can be employed to a general transport system, but some details merit further improvements. A better experimental formula for the travel time in terms of the freight flow on links in railway and inland waterways, instead of the BPR function as (3), can characterize more features of different modalities. In addition, we employed the total travel time as travel cost for this case study, while different definitions of costs, e.g., CO_2 emissions [10], could exhibit different results.

15

Acknowledgement

References

[1] H. R. TO, M. M. Barker, White paper: European Transport Policy for 2010: time to decide (2001).

[2] M. Zhang, A. J. Pel, Synchromodal hinterland freight transport: Model study for the port of Rotterdam, Journal of Transport Geography 52 (2016) 1–10.

[3] European Conference of Ministers of Transport, Terminology on combined transport, 1993.

[4] Logistiek, Topteam, Partituur naar de top. Adviesrapport Topteam Logistiek (2011).

[5] B. van Riessen, R. R. Negenborn, R. Dekker, Synchromodal container transportation: an overview of current topics and research opportunities, in: International conference on computational logistics, Springer, 2015, pp. 386–397.

[6] S. Boccaletti, V. Latora, Y. Moreno, M. Chavez, D.-U. Hwang, Complex networks: Structure and dynamics, Physics Reports 424 (4-5) (2006) 175–308.

[7] Å. J. Holmgren, A framework for vulnerability assessment of electric power systems, in: Critical Infrastructure, Springer, 2007, pp. 31–55.

[8] P. Van Mieghem, C. Doerr, H. Wang, J. M. Hernandez, D. Hutchison, M. Karaliopoulos, R. Kooij, A framework for computing topological network robustness, Delft University of Technology, Report20101218.

[9] J. L. Sullivan, D. C. Novak, L. Aultman-Hall, D. M. Scott, Identifying critical road segments and measuring system-wide robustness in transportation networks with isolating links: A link-based capacity-reduction approach, Transportation Research Part A: Policy and Practice 44 (5) (2010) 323–336.

[10] M. Zhang, B. Wiegmans, L. Tavasszy, Optimization of multimodal networks including environmental costs: A model and findings for transport policy, Computers in Industry 64 (2) (2013) 136–145.

[11] P. Erdős, A. Rényi, On random graphs, Publicationes Mathematicae 6 (1959) 290–297.

[12] D. S. Callaway, M. E. Newman, S. H. Strogatz, D. J. Watts, Network robustness and fragility: Percolation on random graphs, Physical review letters 85 (25) (2000) 5468.

[13] P. Van Mieghem, Interconnectivity structure of a general interdependent network, Physical Review E 93 (4) (2016) 042305.

[14] Y. Koç, M. Warnier, P. Van Mieghem, R. E. Kooij, F. M. Brazier, A topological investigation of phase transitions of cascading failures in power grids, Physica A: Statistical Mechanics and its Applications 415 (2014) 273–284.

[15] P. Demeester, M. Gryseels, A. Autenrieth, C. Brianza, L. Castagna, G. Signorelli, R. Clemenfe, M. Ravera, A. Jajszczyk, D. Janukowicz, et al., Resilience in multilayer networks, IEEE Communications Magazine 37 (8) (1999) 70–76.

[16] S. V. Buldyrev, R. Parshani, G. Paul, H. E. Stanley, S. Havlin, Catastrophic cascade of failures in interdependent networks, Nature 464 (7291) (2010) 1025.

[17] M. De Domenico, A. Solé-Ribalta, S. Gómez, A. Arenas, Navigability of interconnected networks under random failures, Proceedings of the National Academy of Sciences 111 (23) (2014) 8351–8356.

[18] A. A. Ganin, M. Kitsak, D. Marchese, J. M. Keisler, T. Seager, I. Linkov, Resilience and efficiency in transportation networks, Science Advances 3 (12) (2017) e1701079.

[19] S. C. Dafermos, F. T. Sparrow, The traffic assignment problem for a general network, Journal of Research of the National Bureau of Standards B 73 (2) (1969) 91–118.

[20] T. G. Crainic, J. M. Rousseau, Multicommodity, multimode freight transportation: A general modeling and algorithmic framework for the service network design problem, Transportation Research Part B: Methodological 20 (3) (1986) 225–242.

[21] S. Çolak, A. Lima, M. C. González, Understanding congested travel in urban areas, Nature Communications 7 (2016) 10793.

[22] Z. He, P. Sun, P. Van Mieghem, Topological approach to measure network recoverability, in: 11th International Workshop on Resilient Networks Design and Modeling (RNDM), IEEE, 2019.

[23] C. Wan, Z. Yang, D. Zhang, X. Yan, S. Fan, Resilience in transportation systems: A systematic review and future directions, Transport Reviews 38 (4) (2018) 479–498.

[24] Y. Zhou, J. Wang, H. Yang, Resilience of transportation systems: concepts and comprehensive review, IEEE Transactions on Intelligent Transportation Systems.

[25] T. Logistiek, Partituur naar de top: Adviesrapport topteam logistiek. p. 2011.

[26] D. I. for Advanced Logistics, Synchromodal transport.

[27] G. Bocewicz, Robustness of multimodal transportation networks, Eksploatacja i Niezawodność 16.

[28] R. Nair, H. Avetisyan, E. Miller-Hooks, Resilience framework for ports and other intermodal components, Transportation Research Record 2166 (1) (2010) 54–65.

[29] H. Chen, K. Cullinane, N. Liu, Developing a model for measuring the resilience of a port-hinterland container transportation network, Transportation Research Part E: Logistics and Transportation Review 97 (2017) 282–301.

[30] I. Stamos, E. Mitsakis, J. M. Salanova, G. Aifadopoulou, Impact assessment of extreme weather events on transport networks: A data-driven approach, Transportation Research Part D: Transport and Environment 34 (2015) 168–178.

[31] M. Darayi, K. Barker, J. R. Santos, Component importance measures for multi-industry vulnerability of a freight transportation network, Networks and Spatial Economics 17 (4) (2017) 1111–1136.

[32] A. Marzuoli, E. Boidot, P. Colomar, M. Guerpillon, E. Feron, A. Bayen, M. Hansen, Improving disruption management with multimodal collaborative decision-making: A case study of the asiana crash and lessons learned, IEEE Transactions on Intelligent Transportation Systems 17 (10) (2016) 2699–2717.

[33] A. Nagurney, Q. Qiang, A network efficiency measure for congested networks, EPL (Europhysics Letters) 79 (3) (2007) 38005.

[34] Y. Zhou, J. Wang, Critical link analysis for urban transportation systems, IEEE Transactions on Intelligent Transportation Systems 19 (2) (2017) 402–415.

[35] M. Taylor, Vulnerability analysis for transportation networks, Elsevier, 2017.

[36] B. Berche, C. Von Ferber, T. Holovatch, Y. Holovatch, Resilience of public transport networks against attacks, The European Physical Journal B 71 (1) (2009) 125–137.

[37] L.-G. Mattsson, E. Jenelius, Vulnerability and resilience of transport systems – A discussion of recent research, Transportation Research Part A: Policy and Practice 81 (2015) 16–34.

[38] E. Rodríguez-Núñez, J. C. García-Palomares, Measuring the vulnerability of public transport networks, Journal of Transport Geography 35 (2014) 50–63.

[39] H. Al-Deek, E. B. Emam, New methodology for estimating reliability in transportation networks with degraded link capacities, Journal of Intelligent Transportation Systems 10 (3) (2006) 117–129.

[40] A. Chen, H. Yang, H. K. Lo, W. H. Tang, Capacity reliability of a road network: an assessment methodology and numerical results, Transportation Research Part B: Methodological 36 (3) (2002) 225–252.

[41] O. Cats, G. J. Koppenol, M. Warnier, Robustness assessment of link capacity reduction for complex networks: Application for public transport systems, Reliability Engineering & System Safety 167 (2017) 544–553.

[42] A. Asadabadi, E. Miller-Hooks, Assessing strategies for protecting transportation infrastructure from an uncertain climate future, Transportation Research Part A: Policy and Practice 105 (2017) 27–41.

[43] W. van Dam, Robustness analysis of the Dutch synchromodal freight transport network: Simulating disruptions on a macroscopic graph model.
URL http://resolver.tudelft.nl/uuid:ed5af468-4555-4018-8463-43165db2775f

[44] F. Southworth, B. E. Peterson, Intermodal and international freight network modeling, Transportation Research Part C: Emerging Technologies 8 (1-6) (2000) 147–166.

[45] S. Trajanovski, J. Martín-Hernández, W. Winterbach, P. Van Mieghem, Robustness envelopes of networks, Journal of Complex Networks 1 (1) (2013) 44–62.

[46] D. M. Scott, D. C. Novak, L. Aultman-Hall, F. Guo, Network robustness index: A new method for identifying critical links and evaluating the performance of transportation networks, Journal of Transport Geography 14 (3) (2006) 215–227.

[47] M. Patriksson, The traffic assignment problem: models and methods, Courier Dover Publications, 2015.

[48] R. Bellman, On a routing problem, Quarterly of Applied Mathematics 16 (1) (1958) 87–90.

[49] J. R. Correa, A. S. Schulz, N. E. Stier-Moses, Selfish routing in capacitated networks, Mathematics of Operations Research 29 (4) (2004) 961–976.

[50] J. G. Wardrop, Road paper. Some theoretical aspects of road traffic research., Proceedings of the institution of civil engineers 1 (3) (1952) 325–362.

[51] M. Fukushima, A modified Frank-Wolfe algorithm for solving the traffic assignment problem, Transportation Research Part B: Methodological 18 (2) (1984) 169–177.

[52] J. N. Prashker, S. Bekhor, Some observations on stochastic user equilibrium and system optimum of traffic assignment, Transportation Research Part B: Methodological 34 (4) (2000) 277–291.

[53] P. A. Chen, D. Kempe, Altruism, selfishness, and spite in traffic routing, in: Proceedings of the 9th ACM conference on Electronic Commerce, ACM, 2008, pp. 140–149.

[54] R. L. Tobin, T. L. Friesz, Sensitivity analysis for equilibrium network flow, Transportation Science 22 (4) (1988) 242–250.

[55] M. Patriksson, Sensitivity analysis of traffic equilibria, Transportation Science 38 (3) (2004) 258–281.

[56] O. Cats, Topological evolution of a metropolitan rail transport network: The case of Stockholm, Journal of Transport Geography 62 (2017) 172–183.

[57] D. Braess, Über ein paradoxon aus der verkehrsplanung, Unternehmensforschung 12 (1) (1968) 258–268.

[58] L. Lü, D. Chen, X. Ren, Q. Zhang, Y. Zhang, T. Zhou, Vital nodes identification in complex networks, Physics Reports 650 (2016) 1–63.

[59] P. Van Mieghem, Performance analysis of complex networks and systems, Cambridge University Press, 2014.

[60] P. Van Mieghem, K. Devriendt, H. Cetinay, Pseudoinverse of the Laplacian and best spreader node in a network, Physical Review E 96 (3) (2017) 032311.

[61] L. Zhang, G. Zeng, D. Li, H.-J. Huang, H. E. Stanley, S. Havlin, Scale-free resilience of real traffic jams, Proceedings of the National Academy of Sciences 116 (18) (2019) 8673–8678.